Available at www.sciencedirect.com

ScienceDirect

journal homepage: www.elsevier.com/locate/he

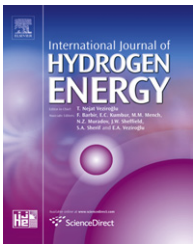

Pd nanoparticles deposited on vertically aligned carbon nanotubes grown on carbon paper for formic acid oxidation

Jiajun Wang [a,b], *Geping Yin* [a,*], *Yougui Chen* [b], *Ruying Li* [b], *Xueliang Sun* [b,**]

[a] *School of Chemical Engineering and Technology, Harbin Institute of Technology, Xi-dazhi Street, Harbin 150001, China*
[b] *Department of Mechanical and Materials Engineering, The University of Western Ontario, London, Ontario, Canada N6A 5B9*

ARTICLE INFO

Article history:
Received 17 April 2009
Received in revised form
13 July 2009
Accepted 23 July 2009
Available online 15 August 2009

Keywords:
Formic acid fuel cell
Vertically aligned carbon nanotubes
Pd nanoparticles
Three-dimensional structure

ABSTRACT

Vertically aligned carbon nanotubes (VACNTs) grown on carbon paper were obtained by the spray pyrolysis method and highly dispersed Pd nanoparticles were deposited on VACNTs by the wet chemical method. For comparison, the entangled carbon nanotubes (ECNTs) and Vulcan XC-72 based electrodes were fabricated by brush painting the corresponding Pd/ECNTs and Pd/XC-72 catalysts on carbon paper, respectively. Compared with Pd deposition on the entangled carbon nanotubes (ECNTs) and Vulcan XC-72 electrodes, the VACNTs electrode exhibited higher activity for formic acid oxidation, which is mainly due to the three-dimensional structure and better conductive paths in the VACNTs electrode, as well as higher Pd utilization.

1. Introduction

Recently, direct formic acid fuel cells are receiving more attention due to higher theoretical open circuit potential and lower fuel crossover through the Nafion membrane, compared to direct methanol fuel cells [1–3]. Despite the advantages, the low catalytic activity and cost issue of the noble catalyst have to be overcome before commercialization. In recent years, Pd catalysts were found to show superior catalytic activity for formic acid oxidation reaction compared to Pt catalysts [4,5]. To further increase the catalytic activity and decrease the noble metal loading, considerable efforts were devoted to develop highly dispersed Pd nanoparticles on the supporting material. The commercial Vulcan XC-72 (XC-72) carbon black has been widely used as the support for Pd catalyst, but many Pd nanoparticles can be trapped in the micropores and deep cracks of the carbon black and thus do not contribute to the triple-phase boundary [6]. Besides, XC-72 may have serious corrosion problems in operation of the fuel cell [7,8].

Carbon nanotubes have been used as an alternative support for noble metal catalysts in polymer electrolyte membrane fuel cells (PEMFCs) due to their unique tubular structure, high surface area, and high corrosion resistance [9,10]. Recent reports have shown that Pd based nanoparticles supported on CNTs exhibited excellent properties for formic acid oxidation [11]. However, a high contact resistance [12] between carbon nanotubes and current collectors is introduced by the conventional electrode preparation method, which involves dispersing the Pt/CNTs catalyst ink and brush painting or spraying it on carbon paper. Furthermore, entangled carbon nanotubes (ECNTs) electrodes possess irregular pore structures that would not facilitate the fast transfer of the electrons, thus limiting the performance improvement of CNTs. To make full use of the superior performance of carbon nanotubes, the fabrication of novel carbon nanotubes based electrode with high performance remains a challenge.

Vertically aligned carbon nanotubes (VACNTs) are excellent candidates for the fabrication of CNTs electrodes due to

* *Corresponding author*. Tel.: +86 451 86413707; fax: +86 451 86413707.
** *Corresponding author*. Tel.: +1 519 661 2111x87759; fax: +1 519 661 3020.
E-mail addresses: yingphit@hit.edu.cn (G. Yin), xsun@eng.uwo.ca (X. Sun).
0360-3199/$ – see front matter © 2009 Professor T. Nejat Veziroglu. Published by Elsevier Ltd. All rights reserved.
doi:10.1016/j.ijhydene.2009.07.082

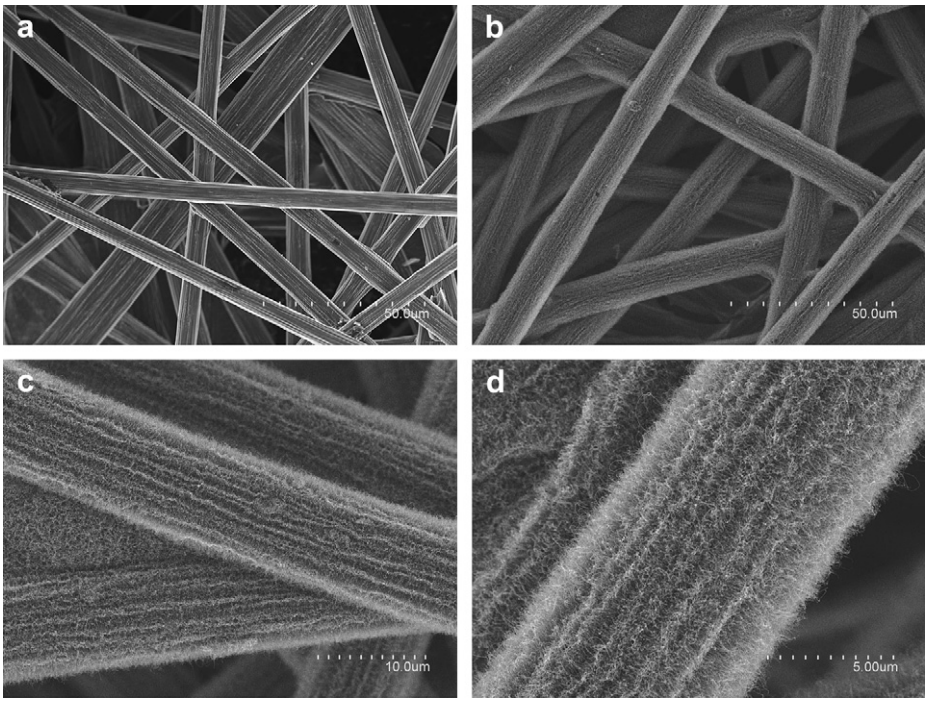

Fig. 1 – SEM images of original carbon fiber on carbon paper (a) and VACNTs on carbon paper with low (b) and high magnifications(c,d).

the more regular pore structures and conductive paths, which allow faster rates of electron transfer [13,14]. In this paper, VACNTs grown on carbon paper were prepared by the spray pyrolysis method and highly dispersed Pd nanoparticles were deposited on VACNTs by the wet chemical method. For comparison, the ECNTs powder was scratched from CNTs forest growth on carbon paper for the fabrication of Pd/ECNTs electrode. The performances of the two electrodes were also compared with the Vulcan XC-72 based Pd electrode.

2. Experimental

2.1. *Preparation of carbon nanotubes*

The growth of VACNTs was carried out directly on carbon paper by the spray pyrolysis method [15]. Briefly, ferrocene was used as the catalyst and dissolved in alcohol (which acted as the carbon source). Prior to the growth of carbon nanotubes, argon was introduced into the quartz tube to eliminate the air. Then the system was heated and the solution containing the catalyst and carbon source was introduced into it at a flow rate of 200 sccm. The synthesis process was performed at 850 °C for 5 min. The three-dimensional VACNTs on carbon paper were thus obtained. The ECNTs powder was obtained by scratching from the CNTs forest grown on carbon paper. The commercial XC-72 powder was purchased from Cabot Corporation for comparison.

2.2. *Deposition of Pd and electrode preparation*

Prior to the Pd deposition, the ECNTs powder and VACNTs electrode were modified by means of the acidic treatment to remove the metal remains and form more active sites, allowing easier anchoring of the Pd nanoparticles. For the deposition of Pd on the VACNTs electrode, the conventional wet chemical method was carried out on the sample. A typical preparation consists of the following steps: 0.15 ml of an aqueous solution of 200 mM Na_2PdCl_4 was mixed with 100 ml H_2O in a beaker, and the VACNTs electrode was suspended in the Pd precursor solution, followed by the addition of 6 mg trisodium citrate. After several minutes, a mixture solution of trisodium citrate and $NaBH_4$ was injected into the beaker at a low speed. The reaction was allowed to proceed for 1 h with constant stirring at room temperature. The resulting electrode was washed with distilled water and dried in vacuum at 60 °C overnight.

The powder Pd/ECNTs and Pd/XC-72 catalysts were both prepared using the same method, which was as follows: firstly, 10 mg of Pd catalyst was ultrasonically mixed with 0.5 ml Nafion solution (5 wt%) and 2.5 ml isopropanol; second, the catalyst ink was brush painted onto the carbon paper (E-TEK, a division of BASF Fuel Cells, Somerset, NJ); then the electrode was dried in vacuum at 60 °C.

2.3. *Electrochemical measurements*

Electrochemical measurements were performed at a standard three-electrode electrochemical cell with CHI 600C electrochemical working station. A conventional three-electrode cell was used, including an Ag/AgCl (saturated KCl) electrode as reference electrode, a platinum wire as counter electrode, and the as-prepared electrodes as working electrodes. Cyclic voltammeter (CV) and chronoamperometry (CA) experiments

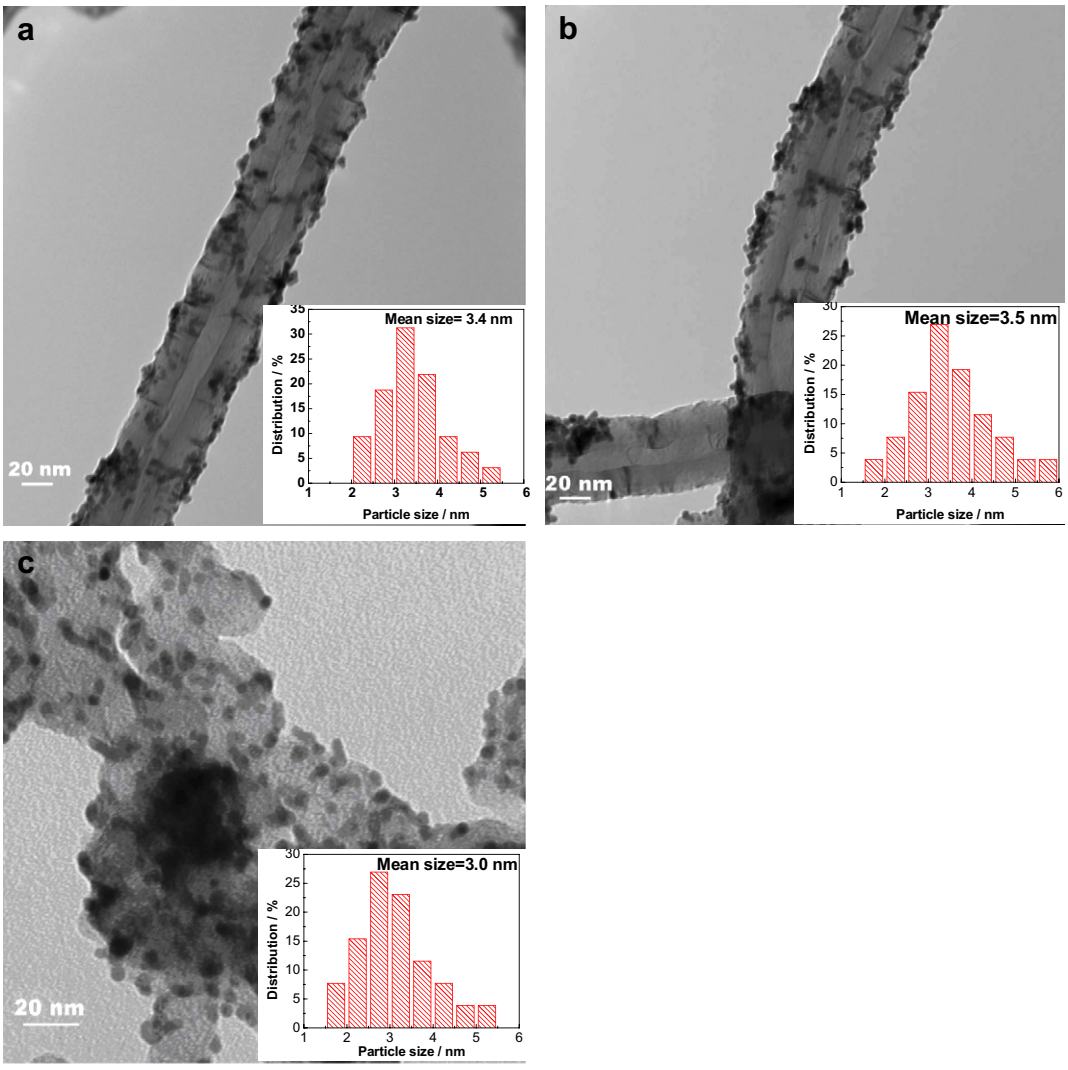

Fig. 2 – TEM images of Pd nanoparticles on VACNTs (a), ECNTs (b), and XC-72 (c).

were conducted in N_2 purged in 0.5 mol L^{-1} H_2SO_4 + 0.5 mol L^{-1} HCOOH solutions at 25 °C. CO-striping measurements were carried out by purging CO into the 0.5 M H_2SO_4 solution to allow the complete adsorption of CO onto the catalyst while holding the working electrode at −0.166 V for 30 min. The remaining CO was purged out by flowing Ar for 30 min before measurements were made [16,17].

2.4. *Characterization of the Pd catalysts*

The Pd loading in the electrodes was determined by inductively coupled plasma-optical emission spectroscopy (ICP-OES). The morphologies for carbon nanotubes and Pd catalysts were obtained with a field emission scanning electron microscope (Hitachi S-4800) and transmission electron microscopy (TEM) (Philips CM10).

3. Results and discussion

The Pd loadings of the electrodes were determined by ICP-OES analysis. The results obtained were 0.13, 0.15, and 0.16 mg cm^{-2} for the Pd/VACNTs, Pd/ECNTs, and Pd/XC-72 electrodes, respectively.

Fig. 1 shows the SEM images of the aligned carbon nanotubes grown directly on the carbon paper. As shown in the images, the VACNTs with a high density were oriented perpendicularly to the carbon fiber. Moreover, all the carbon fibers are uniformly covered by a forest of carbon nanotubes of about 3 μm length.

Fig. 2 represents the TEM images and the corresponding histograms of the particle size distributions for the three Pd

Table 1 – Comparison of particle size, ESA, CSA, and Pd utilization of various catalysts.

Catalysts	Particle size (TEM, nm)	ESA (cm^2/mg Pd)	CSA (cm^2/mg Pd)	η_{Pd} (%)
Pd/VACNTs	3.4	916.7	1470.5	62.3
Pd/ECNTs	3.5	654.2	1428.5	45.8
Pd/XC-72	3.0	525.0	1666.7	31.5

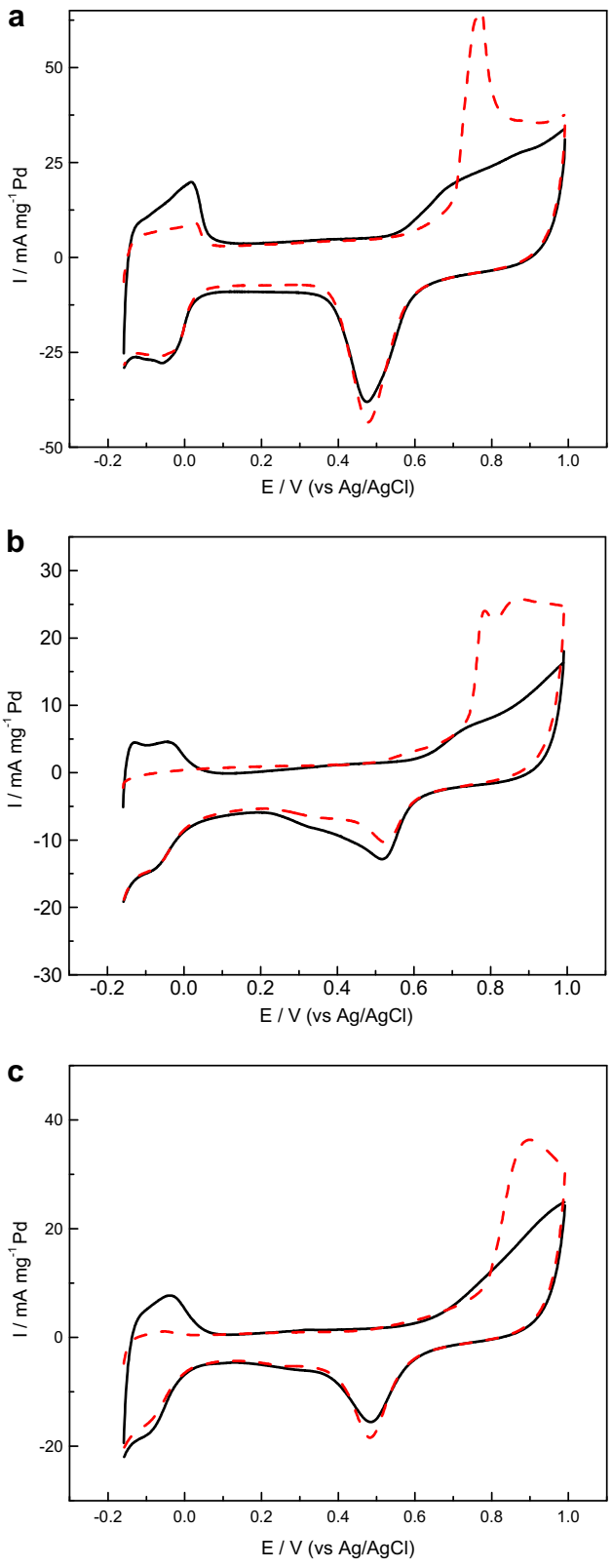

Fig. 3 – CO-stripping voltammograms for Pd/VACNTs (a), Pd/ECNTs (b), and Pd/XC-72 (c) at a scan rate of 10 mV s^{-1}.

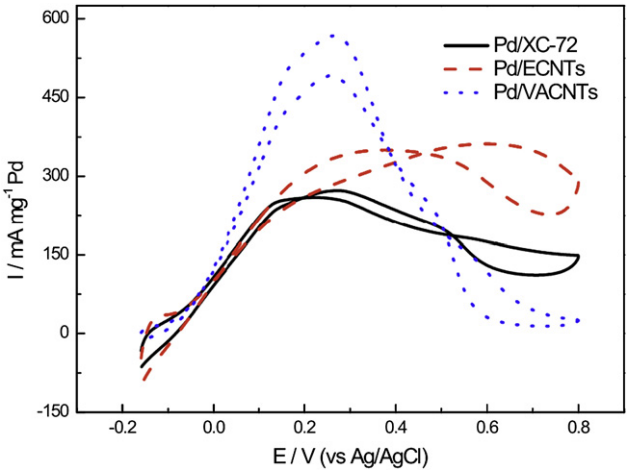

Fig. 4 – Cyclic voltammograms of Pd/VACNTs, Pd/ECNTs, and Pd/XC-72 electrodes in 0.5 M H_2SO_4 containing 0.5 M HCOOH solutions at a scan rate of 20 mV s^{-1}.

catalysts. As shown in Fig. 2a, the Pd nanoparticles with uniform size are well dispersed on the VACNTs. The small and uniform Pd nanopaticle sizes are due to the stabilizing effect of citrate during the preparation process. Similar results can also be obtained in the Pd/ECNTs sample (see Fig. 2b). From the TEM images in Fig. 2b, it can be seen that the Pd nanoparticles are also well dispersed on the ECNTs, and the particle size is also uniform. The similar Pd particle size and dispersion on the two CNTs samples are due to the fact that the carbon nanotubes supports were prepared in the same synthesis process, as well as the fact that the catalyst preparation method was also the same. Fig. 2c shows the images of Pd/XC-72. The Pd nanoparticles still have a similar size to the other cases, but the nanoparticles are slightly more uniformly dispersed on the carbon particles. The average size of the Pd particles on the catalysts was also obtained by directly measuring over 200 randomly chosen particles from the TEM micrographs, which was listed in Table 1. Clearly, in this study, the citrate stabilizer plays a key role in keeping a similar Pd particle size on the three supports, while the different Pd particles dispersion mainly depends on the carbon support. The slightly lower Pd dispersion on CNTs is mainly due to the inert graphite layers and the

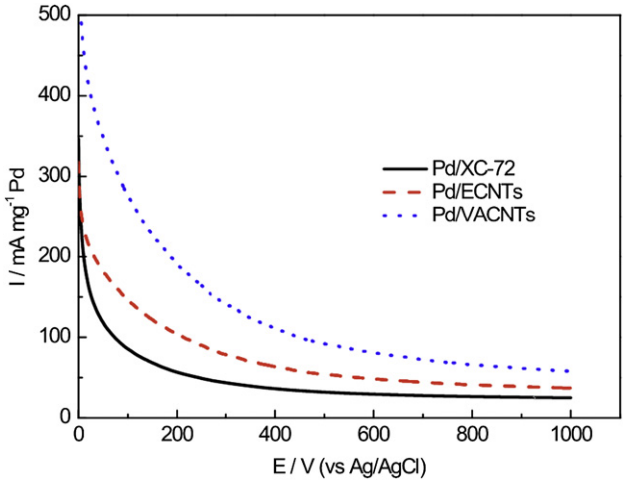

Fig. 5 – Chronoamperometic curves of Pd/VACNTs, Pd/ECNTs, and Pd/XC-72 electrodes in 0.5 M H_2SO_4 containing 0.5 M HCOOH solution.

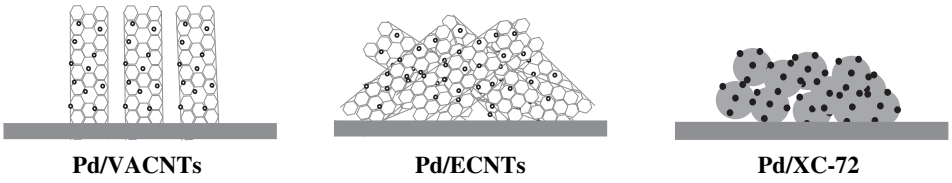

Fig. 6 – Schematic models of the Pd/VACNTs, Pd/ECNTs, and Pd/XC-72 electrodes.

higher surface tension on the CNTs support [18]. Here, the chemical surface areas (CSAs) of these catalysts are calculated from the equation [19]:

$$\mathrm{CSA} = \frac{6}{\rho d} \quad (1)$$

where ρ is the density of Pd (12 g cm^{-3}) and d is the mean diameter of the Pd nanoparticles in the catalysts. The calculated result was also shown in Table 1.

Fig. 3 shows the cyclic voltammograms with and without (dashed and solid curves, respectively) CO adsorption on Pd catalysts in 0.5 M H_2SO_4. The CO-stripping voltammogram is a common technique for determining the electrochemical specific surface area (ESA) of the electrodes through the oxidation of absorbed CO. As shown in Fig. 3, a well-defined CO-stripping peak is obviously found on each sample. The calculated CO-stripping charges are 440, 314, and 252 mC mg^{-1} for the Pd/VACNTs, Pd/ECNTs, and Pd/XC-72 electrodes, respectively. The corresponding ESAs were determined according to the literature [20] and shown in Table 1. From the above ESA and CSA, it is possible to estimate the Pd utilization (η) [21]

$$\eta = \frac{\mathrm{ESA}}{\mathrm{CSA}} \quad (2)$$

The calculation results are shown in Table 1. The result shows that the three-dimensional Pd/VACNTs electrode shows the highest ESA and Pd utilization, while the Pd/XC-72 shows the lowest. As discussed above, the three Pd catalysts have similar Pd nanoparticle size, thus the particle size effect for the ESA of the Pd catalyst can be neglected in this study. The lowest ESA and Pd utilization for the Pd/XC-72 are most likely due to the lower conductivity of the support and the presence of micropores on the XC-72 particles where the Pd nanoparticles may be trapped and become electrochemically inaccessible [22]. Compared with Pd/ECNTs, the higher ESA of Pd/VACNTs is likely due to the fact that the electrode possesses a three-dimensional structure and better conductive paths [14].

Fig. 4 compares the formic acid oxidation activities of the three Pd catalysts in 0.5 M H_2SO_4 containing 0.5 M HCOOH. As shown in Fig. 4, the highest HCOOH oxidation current can be observed in the Pd/VACNT sample, indicating the highest catalytic activity for HCOOH oxidation. The specific mass activities of the Pd/VACNTs, Pd/ECNTs, and Pd/XC-72 calculated from the forward-scan currents were 538, 302, 249 mA mg^{-1} Pd at 0.3 V, respectively. The significant enhancement for the catalytic activity of HCOOH oxidation on the Pd/VACNTs electrode was related to the three-dimensional aligned CNTs electrode structure.

Fig. 5 shows the chronoamperometric curves of the three Pd catalysts at 200 mV in 0.5 M H_2SO_4 containing 0.5 M HCOOH. A decrease in the current density with time is found in each electrode sample. The initial current densities at the applied potential are consistent with the voltammograms in Fig. 3. After the application of the set potential for 1000 s, the current densities for the Pd/VACNTs, Pd/ECNTs, and Pd/XC-72 were 57.9, 35.2, and 26.5 mA mg^{-1} Pd, respectively. The results further demonstrated that the Pd/VACNTs catalyst exhibited the best performance.

Fig. 6 represents the schematic models of the above three electrodes. It can be seen that the conductive paths in the Pd/ECNTs and Pd/XC-72 electrodes are irregular and long. Moreover, some of the Pd nanoparticles are wrapped by the carbon particles or entangled CNTs and cannot be exposed, resulting in low Pd utilization. By comparison, each single carbon nanotube is grown and contacted directly with the carbon fiber on the ECNTs electrode, thus it has a higher conductivity. Furthermore, almost all of the Pd nanoparticles on the surface of VACNTs are well exposed to the electrolyte, which contributes to the higher accessible surface area of Pd. Thus, the Pd/VACNTs electrode exhibits the highest performance and can be used as a good candidate electrode for formic acid fuel cells.

4. Conclusions

VACNTs grown on carbon paper were obtained by the spray pyrolysis method and highly dispersed Pd nanoparticles were well deposited on VACNTs by a wet chemical method. Electrochemical investigation indicated that the three-dimensional Pd/VACNTs electrode exhibited higher catalytic activity for formic acid oxidation, compared with the Pd/ECNTs and Pd/XC-72 electrodes. Thus, VACNTs grown on carbon paper can be used as a more suitable and promising electrode material for formic acid fuel cells.

Acknowledgements

We are in debt to David Tweddell for his kind help and fruitful discussions.

REFERENCES

[1] Yu XW, Pickup PG. Recent advances in direct formic acid fuel cells (DFAFC). J Power Sources 2008;177:124–32.
[2] Rice C, Ha S, Masel RI, Wieckowski A. Catalysts for direct formic acid fuel cells. J Power Sources 2003;115:229–35.

[3] Hotza D, Costa JSD. Fuel cells development and hydrogen production from renewable resources in Brazil. Int J Hydrogen Energy 2008;33(19):4915–35.
[4] Zhang XG, Toshihide A, Yasushi M, Kiyochika Y, Yoshio T. Electrocatalytic oxidation of formic acid on ultrafine palladium particles supported on a glass carbon. Electrochim Acta 1995:1889–97.
[5] Zhu YM, Zakia K, Masel RI. The behavior of palladium catalysts in direct formic acid fuel cells. J Power Sources 2005;139:15–20.
[6] Shao YY, Yin GP, Wang JJ, Gao YZ, Shi PF. Multi-walled carbon nanotubes based Pt electrodes prepared with in situ ion exchange method for oxygen reduction. J Power Sources 2006;161(1):47–53.
[7] Wang JJ, Yin GP, Shao YY, Zhang S, Wang ZB, Gao YZ. Effect of carbon black support corrosion on the durability of Pt/C catalyst. J Power Sources 2007;171:331–9.
[8] Wang ZB, Zuo PJ, Chu YY, Shao YY, Yin GP. Durability studies on performance degradation of Pt/C catalysts of proton exchange membrane fuel cell. Int J Hydrogen Energy 2009; 34(10):4387–94.
[9] Shao YY, Yin GP, Zhang J, Gao YZ. Comparative investigation of the resistance to electrochemical oxidation of carbon black and carbon nanotubes in aqueous sulfuric acid solution. Electrochim Acta 2006;51:5853–7.
[10] Zhang S, Yuan X, Wang H, Mérida W, Zhu H, Shen J, et al. A review of accelerated stress tests of MEA durability in PEM fuel cells. Int J Hydrogen Energy 2009;34(1):388–404.
[11] Yang SD, Zhang XG, Mi HY, Ye XG. Pd nanoparticles supported on functionalized multi-walled carbon nanotubes (MWCNTs) and electrooxidation for formic acid. J Power Sources 2008;175:26–32.
[12] Rauhe BR, Mclarnon FR, Cairns EJ. Direct anodic oxidation of methanol on supported platinum/ruthenium catalyst in aqueous cesium carbonate. J Electrochem Soc 1995;142:1073–84.
[13] Ahn HJ, Moon WJ, Seong TY, Wang DY. Three-dimensional nanostructured carbon nanotube array/PtRu nanoparticle electrodes for micro-fuel cells. Electrochem Commun 2009; 11:635–8.
[14] Zhang H, Cao GP, Yang YS, Gu ZN. Comparison between electrochemical properties of aligned carbon nanotube array and entangled carbon nanotube electrodes. J Electrochem Soc 2008;155(2):K19–22.
[15] Yang Z, Chen XH, Nie HG, Zhang K, Li WH, Yi B, et al. Direct synthesis of ultralong carbon nanotube bundles by spray pyrolysis and investigation of growth mechanism. Nanotechnology 2008;19:085606.
[16] Zhou WJ, Lee JY. Highly active core-shell Au–Pd catalyst for formic acid electrooxidation. Electrochem Commun 2007;9: 1725–9.
[17] Wu JF, Yuan XZ, Wang HJ, Blanco M, Martin JJ, Zhang JJ. Diagnostic tools in PEM fuel cell research: part I electrochemical techniques. Int J Hydrogen Energy 2008; 33(6):1735–46.
[18] Li XG, Hsing IM. The effect of the Pt deposition method and the support on Pt dispersion on carbon nanotubes. Electrochim Acta 2006;51:5250–8.
[19] Hsieh CT, Lin JY, Wei JL. Deposition and electrochemical activity of Pt-based bimetallic nanocatalysts on carbon nanotube electrodes. Int J Hydrogen Energy 2009;34(2): 685–93.
[20] Chaparro AM, Martın AJ, Folgado MA, Gallardo B, Daza L. Comparative analysis of the electroactive area of Pt/C PEMFC electrodes in liquid and solid polymer contact by underpotential hydrogen adsorption/desorption. Int J Hydrogen Energy 2009;34:4838–46.
[21] Lee SK, Kim CH, Cho WC, Kang KS, Park CS, Bae KK. The effect of Pt loading amount on SO2 oxidation reaction in an SO_2-depolarized electrolyzer used in the hybrid sulfur (HyS) process. Int J Hydrogen Energy 2009;34:4701–7.
[22] Saha MS, Li RY, Sun XL, Ye SY. 3-D composite electrodes for high performance PEM fuel cells composed of Pt supported on nitrogen-doped carbon nanotubes grown on carbon paper. Electrochem Commun 2009;11:438–41.